Synthesis and temperature dependent fluorescence properties of nanoscale europium doped yttria derived in presence of tween-80 and β-alanine

Pramod K. Sharma[a],*, M.H. Jilavi[b], H. Schmidt[b], V.K. Varadan[a]

[a]CEEAMD, 712 Earth and Engineering Science Bldg., The Pennsylvania State University, University Park, PA 16802, USA
[b]Institut fuer Neue Materialien, Im Stadtwald, Geb. 43, D-66123 Saarbrucken, Germany

Abstract

A novel procedure for the synthesis of uniform europium doped yttria powder was developed. It was prepared by chemically growth-controlled method in the presence of surface modifier. A mixture of Tween-80 (polyoxyethylene (20) sorbitate) and β-alanine, was used as surface modifier. The obtained powder was pure and highly crystalline. The powder was also examined via Fourier transformation infra red (FTIR) spectroscopy to determine the presence of nitrate ions along with the powder at pre and post calcination. Thermal behavior of the powder was investigated by thermal gravimetric analysis (TGA) and differential thermal analysis (DTA). High Resolution Transmission Microscopy (HRTEM) reveals that the particle size is around 22 nm. Chemical microanalysis of europium doped yttria was made by energy dispersive spectrum analyzer (EDS) attached along with HRTEM and indicated a Y/Eu atomic ratio 2.1. The fluorescence spectra of calcined powder showed that the Eu^{3+} ions were in low symmetry bonding sites in the yttria structure.

.

1. Introduction

The production of reliable and reproducible ceramic materials for high technology applications requires strict control over their powder charcteristics which include chemical homogeneity, low impurity levels, small partcle size, narrow size distribution and freedom from agglomeration [1–5]. A variety of methods e.g. sol–gel, chemical precipitation of precursors in aqueous or organic solutions, thermal decompostion of solutions by spraying technique, high alkaline and hydrothermal precipitation have been proposed for obtaining small, uniform, unagglomerated powders. These methods so-called 'wet chemical methods,' have been found to be successful for number of systems [6–8].

These wet chemical methods start from molecular precursors and consequently have to undergo a growth reaction to form nanosize particles. However, these nanosized particulate systems tend to minimize their surface free energy either by growing to large particles or agglomeration [9]. In order to utilize chemical processes for the synthesis of nanosized powders, these reactions have to be avoided by controlling the thermodynamics of the interfaces within the reacting system. Surface free energy of the particle can be reduced to an appropriate level by the interaction of the surface modifier with the surface of particle [10]. Various oxide powders, including $2ZrO_2$–Yb_2O_3 [11], yttria-stabilized zirconia (YSZ) [12], SiO_2 [13] and ZrO_2 [14] have been produced using different surfactants either in chemical growth control reaction or emulsion based technique.

It is well known that the europium doped yttria has its own importance for its application in scintillation and color TV picture tube. But for the application of this material as advanced material, a regular particle size is a necessary requirement. Therefore, this work presents not only a new method of the preparation of europium doped yttria but also produces the nanoscale particle. Chemical controlled method in presence of surface active modifier (a mixture of tween-80 and β-alanine) was developed for the synthesis of this material. This method can be considered interesting for its simplicity, reproducibility and easy scale up.

.

*Corresponding author.

Nitrates of metal ions were used as initial reagent because nitrates are readily soluble in ethanol. This study also demonstrates the crystallinity and crystallite size of the powders. As this powder was derived by a wet method therefore a detail study was made on the chemical analysis via Fourier transformation infra red (FTIR) spectroscopy and energy dispersive spectrum (EDS) analyzer. This paper also explains the thermal behavior and physical properties of the resultant europium doped yttria powder. The effect of heat treatment on fluorescence behavior of europium ion in doped yttria matrices has also been reported in brief.

2. Experimental

2.1. Preparation of europium doped yttria

Solution (A) was prepared by dissolving a known amount of $Y(NO_3)_3 \cdot 5H_2O$ (0.044 mol) and $Eu(NO_3)_3$ $5H_2O$ (3 mol%) in ethanol. Solution was then stirred for 2 h. Another solution (B) was prepared by dissolving 10 wt% of surface modifier (1:1 mixture of tween-80 and β-alanine) with respect to Eu_2O_3/Y_2O_3 in 50 ml of aqueous ammonium hydroxide solution (pH>10). The resultant solution was stirred again. The solution (A) was then added to the modifier solution drop by drop through burette at the controlled rate (10–15 drops per min) with vigorous stirring. This suspension was stirred continuously for two h. The obtained gel was subjected to centrifuge at the rate of 6000 rpm for 30 min. The aqueous and organic liquids in the centrifugate were removed by drying the gel in the oven at 70°C for 24 h. The powder was heat treated in a box furnace at 450°C for 2 h in an air atmosphere. The final product was a white powder. A schematic diagram of the whole preparation is shown in Fig. 1.

2.2. Characterization

The crystalline phase of the powder was determined by powder X-ray diffraction (XRD) on D-500 Siemens powder diffractometer. The infra red spectra of the sample was recorded on a Fourier-transformation infrared spectrophotometer (Brucker IFS 25). Thermal analysis was carried out on Bähar thermoanalyzer (STA 501) in air from 25°C to 800°C. The particle size of the powder was determined by using microtrac particle size analyzer (UPA 9200). The samples for particle size analysis were prepared by making a powder suspension in the deionized water. The suspension was ultrasonicated for 15 min so that particle should not be settled down.

2.3. Microstructure and nanostructure

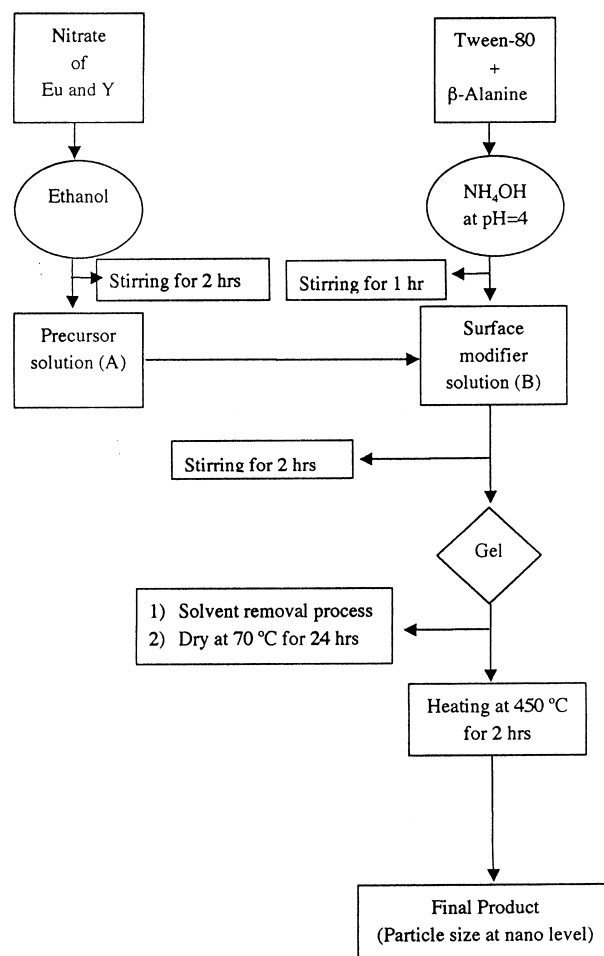The nanostructure of particle was investigated in a high

Fig. 1. A schematic diagram of the powder preparation.

resolution transmission microscope (HRTEM) (Philips CM 200) operated at 200 kV with a line resolution of 1.4. The microscope is equipped with a Si-detector for energy dispersive spectrum (EDS) analysis for the microchemical investigation of TEM sample. For TEM specimen preparation, the copper grid was used which was covered with a very thin film of amorphous carbon for holding the nanosize particles. It also avoids the charge effect during the microscopy examinations. The copper grid was dipped in a suspension of examined solution.

2.4. Fluorescence properties

Pallets of the powder were prepared by a load of 5 tons. A known amount of the powder was used for the pallet formation. The pallet is dried well in the oven at 70°C for 1 h to avoid any moisture. The fluorescence spectra were measured with a Hitachi fluorescence spectrophotometer with a 150 W xenon lamp (3100).
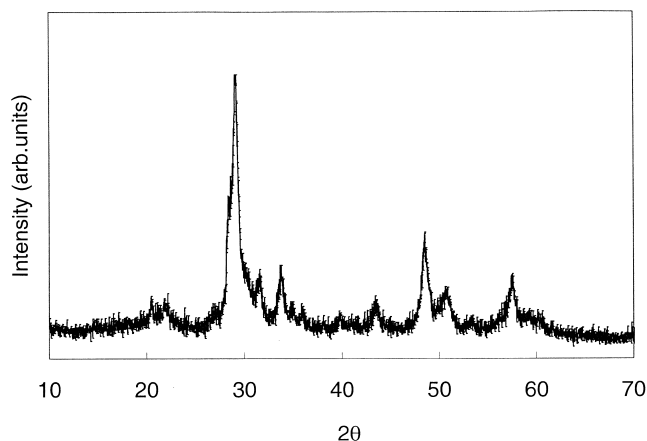
Fig. 2. X-ray diffraction spectra of the powder at 450°C.

3. Results and discussion

3.1. Phase analysis

XRD pattern of europium doped yttria is shown in Fig. 2. The powder obtained by this method is pure and highly crystalline at the temperature 450°C. XRD pattern confirms the absence of any impurity due to precursor. It attributes that the concentration used for europium is sufficient for a complete dissolution as a dopant in yttria.

3.2. Thermal and chemical characterization

Fig. 3 shows typical thermal analysis results for the gel. The dominant thermal process was observed between 100°C to 430°C. DTA showed endothermic and exothermic phenomenon in the similar temperature range. Ther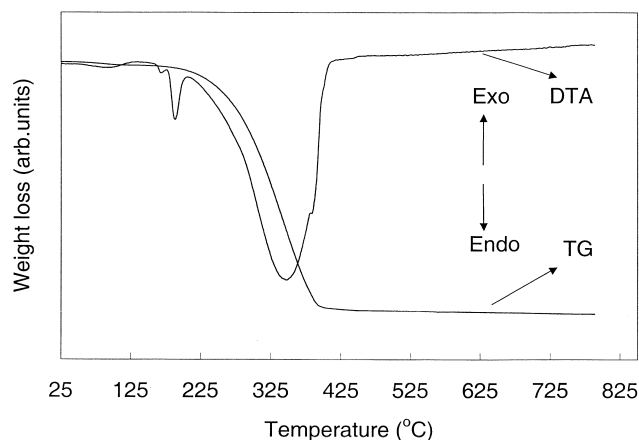e was no further weight loss measured above 430°C. Initial weight loss due to dehydration corresponded to a two step endothermic process in which physical adsorbed water was assumed to be lost before more strongly held chemisorbed water that was surface hydroxyl group and water coordinated to the metal ions [15]. The DTA curve shows one more endotherm at 370°C, which can be attributed to the partial dehydroxilation [16]. An exothermic peak between 270°C-320°C was expected which could be assigned for the removal of organic which accompanying with a corresponding weight loss in TG. The absence of any exothermic peak in the DTA curve for the removal of higher molecular weight organic (β-alanine and tween-80) in this temperature range was surprising. Absence of such an exothermic peak may be attributed to the following reason: an exothermic reaction that occurs, but its presence was masked by one of the endothermic peak associated with a hydroxyl group since the temperature region coincides with the endotherm.

Fig. 4(a) and 4(b) show the FTIR spectra of the powders dried at room temperature and calcined at 450°C. In the Fig. 4(a) a broad peak apparent at 3360 cm^{-1} and a shoulder at 1685 cm^{-1}, can be attributed to -OH stretching and bending respectively. The peak at 2956 cm^{-1} was represented the stretching frequency of CH bond. The peaks at 1380 and 1450 cm^{-1} were assigned to the stretching of C=C and C-C bonds. While the peaks at 1515 cm^{-1} and 1420 cm^{-1} were due to the C–O bond stretching and bending. The N-O stretching were found at 1560, 1030 and 820 cm^{-1}. FTIR spectrum of the dried gel showed that the major constituents of the organic matter, have originated apparently from tween-80, β-alanine and ethanol. Peaks due to the organic matter, have disappeared when the gel was heated at 450°C (refer to Fig. 4(b)). The elimination of the organic matter at this stage resembles the TG/DTA results. But the major peaks due to N-O were retained. Since the powder was prepared at temperatures
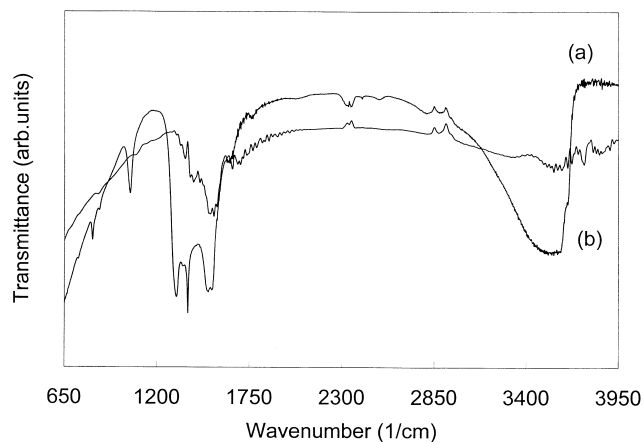

Fig. 3. TG-DTA curve of dried powder.

Fig. 4. FTIR spectra of (a) dried gel and (b) heat treated at 450°C.
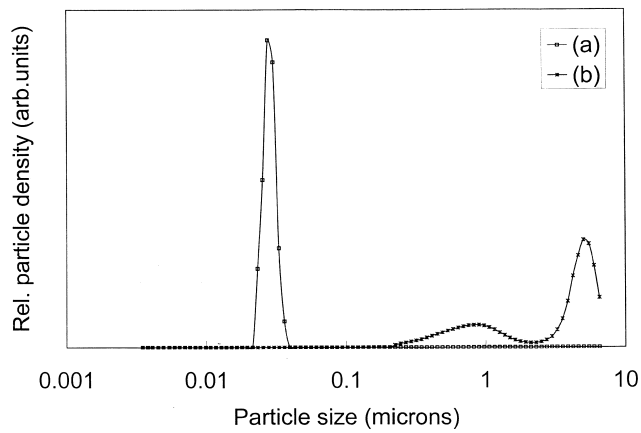
Fig. 5. Particle size distribution of the powder with modifier conc. (a) 0wt.% and (b) 10wt.%.

<450°C, it was expected that the powder obtained was a simple metal oxide with nitrate ions on the surface as indicated by DTA/TG analysis.

3.3. Particle and morphological studies

Fig. 5 shows the particle size distribution (PSD), of the powders with and without modifier. A bimodal behavior of the PSD is observed when the powder synthesized in absence of modifier. The powder shows a broad PSD with maxima at ≈6 μm. It is seen to a monomodal behavior over the range from 19 to 38 nm giving an average particle diameter of 24 nm for the powder with modifier. The observed particle size distribution is narrow. The powder at temperature 450°C was crystalline with the crystallite sizes of 20.14, 20.78, 18.12, 22.35 and 20.82 nm (refer to Fig. 5). The crystallite size was calculated from Scherrer's equation using the measured full width and half maxima (FWHM) values of peaks [5]. The average crystallite size is therefore, ca 20 nm.

The TEM micrograph reveals the particle size of around 22 nm and an oval morphology as shown in Fig. 6. This particle size has consistency with the value of the particle size determined by UPA method. The microchemical analysis of europium doped yttria was made by EDS (refer to Fig. 7) and indicated a Y/Eu atomic ratio of 2.1. The observed value was higher than that of expected for a Y/Eu (1.45). EDS analysis was also observed for the different particles of the same sample to understand the distribution of europium in the ytrria. This study indicated that the intensity of the europium peak in the EDS was observed to be constant for all the particles in a sample. Therefore, It is an evidence of a homogeneous dispersion of europium within the yttria.
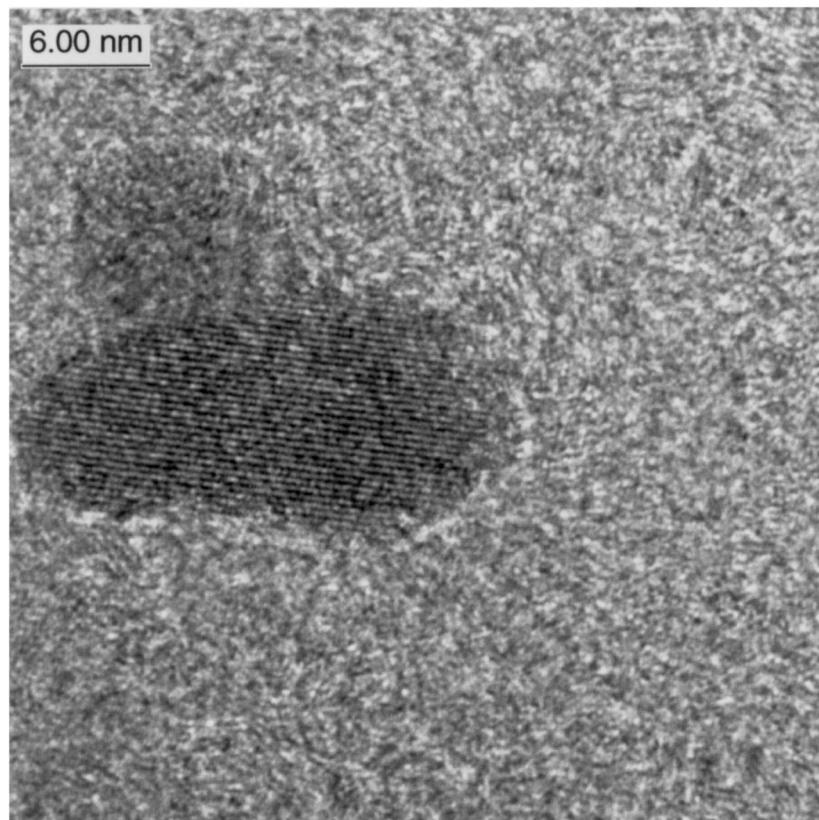

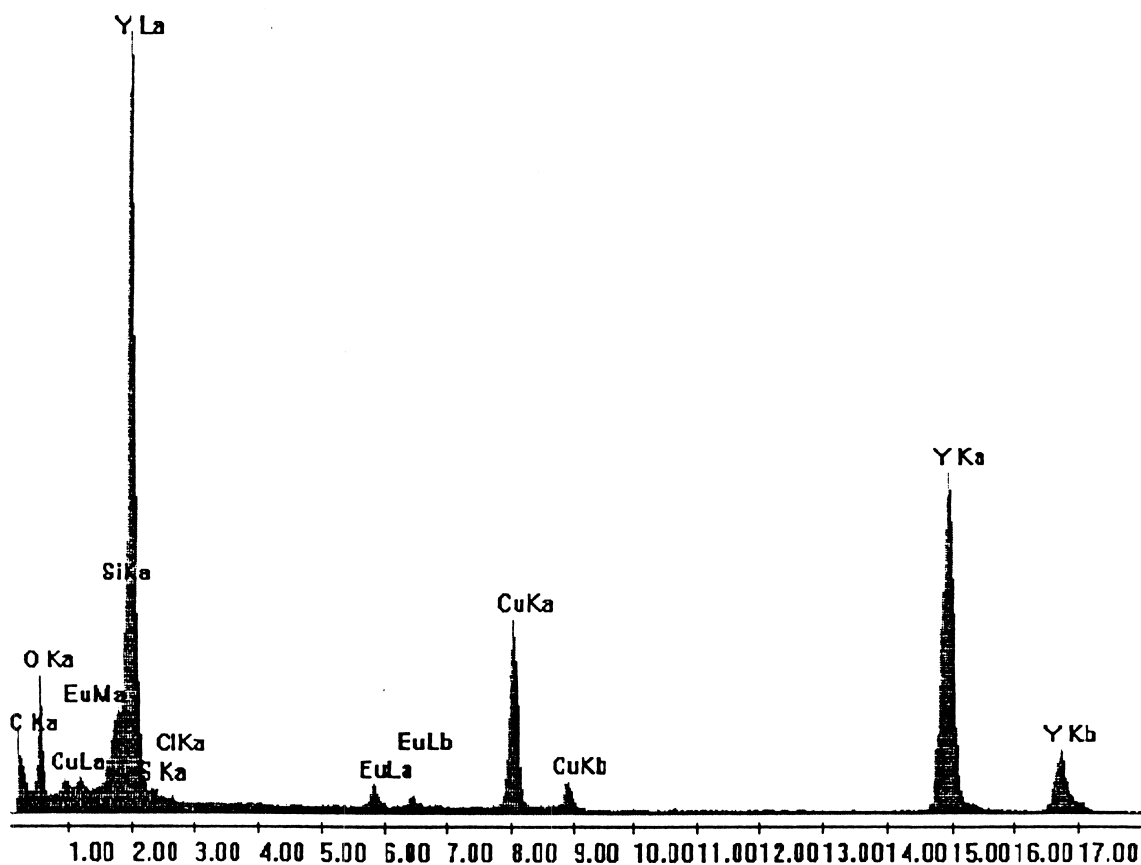Fig. 6. HRTEM micrograph of europium doped yitrria powder at 450°C. Background is an amorphous carbon layer.

Fig. 7. EDS of europium doped yitrria.

3.4. Fluorescence properties

A wavelength of 394 nm was used to excite Eu^{3+} ions into the $^5D_0$ energy level manifold. Figs. 8 and 9 illustrate the emission spectral evolution of the transition of the europium based yttria powder at pre and post calcination. The intensity ratio of the 594 nm emission band corre-sponding to $^5D_0 \rightarrow {}^7F_1$ transition of Eu^{3+} ions to the 614 nm emission band corresponding to the $5D_0 \rightarrow {}^7F_2$ transition in dried gel was very different from that in calcined powders (refer to Figs. 8 and 9). However, a limited shift of wavelength of Eu^{3+} emission band was observed in the different matrices (refer to Fig. 9(a,b)). It indicated that the energy levels of the inner 4f electrons, which are shielded
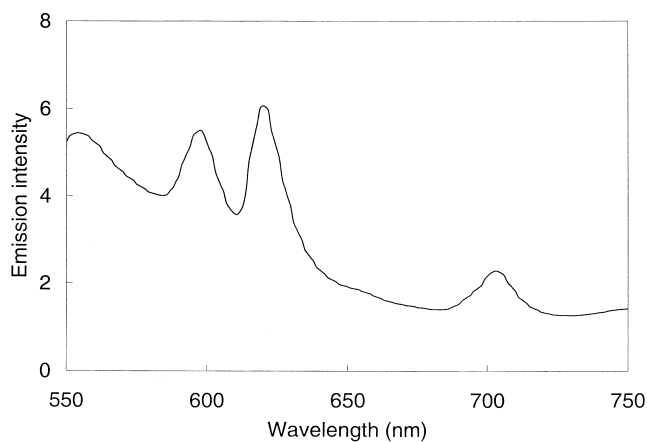

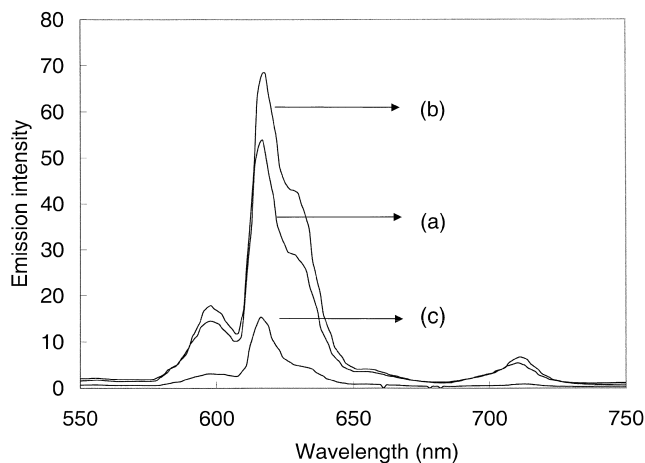Fig. 8. Emission fluorescence spectra of powder under $\lambda_{exc.} \approx 394$ nm at room temperature.

Fig. 9. Emission fluorescence spectra of powder under $\lambda_{exc.} \approx 394$ nm at (a) 350°C, (b) 450°C, and (c) powder without modifier at 450°C.

by the outer 5s, 5d and 5p electrons, were not strongly influenced by the nature of the host lattice into which the Eu^{3+} ions were placed [17].

The emission intensity of the $^5D_0 \rightarrow {}^7F_2$ transition in powder heated at 350°C was stronger than that of the $^5D_0 \rightarrow {}^7F_1$ transition. The same result has also been obtained in the powder heated at temperature 450°C. It is seen in the Fig. 9 that $^5D_0 \rightarrow {}^7F_2$ transition increases several folds with increasing concentration of modifier from 0 wt% to 10 wt% at 450°C. It is known that the intensity of the $^5D_0 \rightarrow {}^7F_2$ transition is strongly affected by the lack of a center of symmetry in the surroundings of Eu^{3+} ions and hence it behaves differently to the local symmetry [18]. When the Eu^{3+} ion were situated at low symmetry sites, the $^5D_0 \rightarrow {}^7F_2$ transition has a greater probability of occurring compared to the $^5D_0 \rightarrow {}^7F_1$ transition [19]. Therefore, the strengthening of the emission intensity of 614 nm band corresponding to the $^5D_0 \rightarrow {}^7F_2$ transition indicates that the Eu^{3+} ions are situated at low symmetry sites in yttria matrix [20]. The fluorescence spectra of the densified powders did not show J-splitting for any of the transition up to the mentioned temperature studied in this work.

4. Conclusion

This study not only offers a new method of processing of europium doped yttria at low temperature but also the particle in nano range. Modifier plays an important role in preparation of nano size particles. By means of FTIR and TG/DTA studies, nitrates have been found to present on the surface of both the dried gel and calcined oxide particles. The Independent measurement of the average particle size of europium doped yttria by HRTEM reveals an average particle diameter 22 nm. The emission intensity of $^5D_0 \rightarrow {}^7F_2$ and $^5D_0 \rightarrow {}^7F_1$ transitions of Eu^{3+} was influenced by heat treatment.

References

[1] Brinker CJ, Scherer GW. Sol–gel science; the physics and chemistry of sol–gel processing, New York: Academic Press Inc, 1990.

[2] Chabi J, Henry M, Zarrouk H, Gharbi N, Livage J. Structural characterization of hybrid materials from Zirconium n-propoxide and 1,2 ethanol. J Non-Cryst Solids 1994;170:1.

[3] Schmidt H. Multifunctional inorganic-organic composite sol–gel coating on glass surface. J Non-Cryst Solids 1994;178:302.

[4] Himmel B, Gerber T, Bürger H, Holzhüter G, Olbertz A. Structural characterization of SiO_2–Al_2O_3 aerogels. J Non-Cryst Solids 1995;186:149.

[5] Jones PF. Fundamental principle's of sol–gel technology, London: The Institute of metals, 1989.

[6] Blanchard CR, Schwab ST. X-ray diffraction analysis of pyrolytic conversion of perhydroposilazane into silicon nitride. J Am Ceram Soc 1994;77:1729.

[7] Sharma PK, Ramanan A, Vasanthacharya NY. Low temperature synthesis of bismuth cuprates. Mater Res Bull 1996;31:913.

[8] Sharma PK, Jilavi MH, Burgard D, Nass R, Schmidt H. Hydrothermal synthesis of Nanosize α-Al_2O_3 from seeded aluminum hydroxide. J Am Ceram Soc 1998;81:2732.

[9] Sharma PK, Nass R, Schmidt H. Effect of solvent, host precursor, dopant concentration and crystallization on the fluorescence properties of Eu (III) doped yttria. Opt Mater 1994;10:161.

[10] Burgard D, Kropf C, Nass R, Schmidt H. Routes to deagglomerated nanopowders by chemical synthesis. Better ceramics through chemistry. Mater Res Soc Symp 1994;346:101.

[11] Kani T, Rhine WE, Bowen HK. Ceramic transaction I. In: Messing GL, Fuller E R, Hausner H, editors, Ceramic powder science, vol. II, New York: American Ceramic Society, 1989, p. 119.

[12] Hardy AR, Gowda G, McMohan TJ, Rlman RE, Rhine WE, Bowen HK. Preparation of oxide powders. In: Mackenzie JD, Ulrich DR, editors, Ultrastructure processing of advanced ceramics, New York: Wiley-Interscience, 1988, p. 407.

[13] Sherif FG, Shyu LJ. Emulsion precipitation of yttria-stabilized zirconia for plasma spray coating. J Am Ceram Soc 1991;74:375.

[14] Ramamurthi SD, Xu ZK, Payne DA. Nanometer-sized ZrO_2 particles prepared by a sol–emulsion–gel method. J Am Ceram Soc 1990;73:2760.

[15] Seaverson LM, Luo S-Q, Chien P-L, McClelland JF. Carbonate associated with hydroxide sol–gel processing of yttria; an inra red spectroscopy study. J Am Ceram Soc 1986;69:423.

[16] Rasmussen MD, Akinc M, Hunter O. Processing of yttria powders derived from hydroxide precursor. Ceram Intern 1985;11:51.

[17] Costa VC, Lochhead MJ, Bary KV. Fluorescence line narrowing study of Eu^{3+} doped sol–gel silica: Effect of modifying cations on the clustering of Eu^{3+}. Chem Mater 1996;6:265.

[18] Omen HJ, Van Dongen AMA. Europium (III) in oxide glasses. Dependence of the emission on spectrum upon glass composition. J Non-Cryst Solids 1989;111:205.

[19] Campostrini R, Carturan G, Ferrari M, Montagna M, Pilla O. Luminescence of Eu^{3+} ion during thermal densification of SiO_2 gel. J Mater Res 1992;7:745.

[20] Devlin K, Kelly BO, Tang JR, McDonagh C, McGilp JF. A structure study of the sol–gel process by optical fluorescence and decay time spectroscopy. J Non-Cryst Solids 1995;135:8.